Final Report

DNA 2802F

October 1971

SCALING PROBLEMS OF WAVE PROPAGATION IN ROCKS

Final Report

By

C. F. PETERSEN, D. R. GRINE, and W. J. MURRI

DEFENSE NUCLEAR AGENCY
WASHINGTON, D.C. 20305

STANFORD RESEARCH INSTITUTE
MENLO PARK, CALIFORNIA 94025

DASA01-69-C-0143

UNCLASSIFIED

Security Classification

DOCUMENT CONTROL DATA - R & D

(Security classification of title, body of abstract and indexing annotation must be entered when the overall report is classified)

1. ORIGINATING ACTIVITY *(Corporate author)*
Stanford Research Institute
Menlo Park, California 94025

2a. REPORT SECURITY CLASSIFICATION
UNCLASSIFIED

2b. GROUP
None

3. REPORT TITLE
SCALING PROBLEMS OF WAVE PROPAGATION IN ROCKS

4. DESCRIPTIVE NOTES *(Type of report and inclusive dates)*
Final Report, May 1, 1969, to September 30, 1970 and March 23 to October 15, 1971

5. AUTHOR(S) *(First name, middle initial, last name)*
Carl F. Petersen, Donald R. Grine, and William J. Murri

6. REPORT DATE
October 1971

7a. TOTAL NO. OF PAGES
60

7b. NO. OF REFS
9

8a. CONTRACT OR GRANT NO.
DASA01-69-C-0143

b. PROJECT NO.
ARPA Order No. 1317

c.

d.

9a. ORIGINATOR'S REPORT NUMBER(S)
PYU 7942

9b. OTHER REPORT NO(S) *(Any other numbers that may be assigned this report)*
DNA 2802F

10. DISTRIBUTION STATEMENT
Approved for public release; distribution unlimited.

11. SUPPLEMENTARY NOTES

12. SPONSORING MILITARY ACTIVITY
Advanced Research Projects Agency
Nuclear Test Detection Office
Washington, D.C. 20301

13. ABSTRACT

Propagation of large-amplitude plane waves was studied in rock specimens from 1/2 to 12 inches thick using in-material piezoresistive stress gages. Sioux quartzite, charcoal black granite, and Coconino sandstone were examined. Good records were obtained in the granite experiments, allowing separation of the precursor from the main wave to be observed at five successive locations in a single experiment. It is concluded that time-dependent effects on wave propagation in quartzite and granite are not significant over these distances. Seven experiments in granite, with dry and water-filled open cracks, displayed the effect of the crack in erasing the precursor. The results show that the presence of a crack volume of a percent or so greatly changes the structure of the precursor. Only a few records were obtained in the sandstone experiments, and these are only partially understood.

DD FORM 1 NOV 68 1473 (PAGE 1)

S/N 0101-807-6801

UNCLASSIFIED

Security Classification

14 KEY WORDS	LINK A		LINK B		LINK C	
	ROLE	WT	ROLE	WT	ROLE	WT
Scaling						
Explosions in rocks						
Constitutive relations of rocks						
Shock-wave propagation						
Geologic materials						

Final Report

DNA 2802F

October 1971

SCALING PROBLEMS OF WAVE PROPAGATION IN ROCKS

This work was supported by the Advanced Research Projects Agency under ARPA Order 1317.

By: C. F. PETERSEN, D. R. GRINE, and W. J. MURRI

Prepared for:

DEFENSE NUCLEAR AGENCY
WASHINGTON, D.C. 20305

CONTRACT DASA01-69-C-0143

SRI Project PYU 7942

Approved by:

G. R. ABRAHAMSON, *Director*
Poulter Laboratory

C. J. COOK, *Executive Director*
Physical Sciences Division

ABSTRACT

Propagation of large-amplitude plane waves was studied in rock specimens from 1/2 to 12 inches thick using in-material piezoresistive stress gages. Sioux quartzite, charcoal black granite, and Coconino sandstone were examined. Good records were obtained in the granite experiments, allowing separation of the precursor from the main wave to be observed at five successive locations in a single experiment. It is concluded that time-dependent effects on wave propagation in quartzite and granite are not significant over these distances. Seven experiments in granite, with dry and water-filled open cracks, displayed the effect of the crack in erasing the precursor. The results show that the presence of a crack volume of a percent or so greatly changes the structure of the precursor. Only a few records were obtained in the sandstone experiments, and these are only partially understood.

FOREWORD

This report expands and revises our previous Final Report, DASA 2579. Since that report was issued, we have conducted five more experiments on granite. These results have been incorporated into the previous report. The work discussed here was performed between May 1, 1969, and September 30, 1970, and between March 23, 1971, and October 15, 1971.

CONTENTS

FIGURES

TABLES

I INTRODUCTION AND SUMMARY

Calculations of stress wave propagation and seismic coupling resulting from detonation of a nuclear or chemical explosive in an earth material require a realistic model of the response of the earth material to an extremely wide range of stress loads, ranging from thousands of kilobars near the explosive source to fractions of a kilobar at great distances from the source.

In the past few years, laboratory shock measurements have been used extensively as input information for computer calculations of stress wave propagation resulting from explosions in earth materials. Although much progress has been made toward understanding this process, there is often great disagreement between field measurements and calculations based on laboratory measurements. Part of the explanation of this discrepancy may be that the thin, homogeneous specimens used in laboratory measurements do not adequately represent field conditions, where large-scale fractures and joints may be common. Also, if time-varying effects are important, the laboratory measurements on thin specimens will not be directly applicable to field studies without an adequate model on which to base long-time extrapolation.

In the present research program, experiments were conducted to study the propagation of large-amplitude plane waves in larger rock specimens than have been used before. The aim was to evaluate the effects of open fractures and the importance of time-varying effects. Hard rocks, (Sioux quartzite and charcoal black granite from Minnesota) and a porous rock (Coconino sandstone, both dry and water-saturated) were studied. Most of the rock specimens were several inches thick, the largest being 12 inches, in contrast to the usual laboratory specimens, which are about 1/4-inch thick. A list of shots fired in the program is given in Table I.

The first six experiments, conducted in Sioux quartzite, were concerned primarily with developing suitable techniques. In-material manganin stress gages were used to record stress-time profiles at intervals of depth in the rock. The large specimens presented difficulties in gage emplacement and recording. The main problem was piezoelectric noise,

Table I

LIST OF SHOTS FIRED

Shot No.	Explosive Train	Specimen	Comments
1	P-120 + 4" TNT	Sioux quartzite	Triggering failed
2	P-120 + 4" TNT	Sioux quartzite	Noisy, data in Table II
3	P-40	Sioux quartzite	Technique Shot, Table II
4	P-40	Sioux quartzite	Technique Shot, Table II
5	P-120 + 4" TNT	Sioux quartzite	Data, Table II
6	P-40	Sioux quartzite	Technique Shot, Table II
7	P-80 + 2" Baratol + 1/2" Al flyer	Dry Coconino sandstone	Technique Shot
8	P-80 + 2" Baratol + 1/2" Al flyer	Wet Coconino sandstone	Technique Shot
9	P-80 + 2" Baratol + 1/2" Al flyer	Dry Coconino sandstone	Data, Table V
10	P-80 + 2" Baratol + 1/2" Al flyer	Wet Coconino sandstone	No records
11	P-40	Granite	Technique Shot
12	P-120 + 4" Comp. B	Granite	Data, Table III and IV
13	P-120 + 4" Comp. B.	Granite	Data, Table III
14	P-120 + 4" Comp. B	Granite	Data, Table III
15	P-120 + 4" Comp. B	Granite	Data, Table III
16	Mousetrap Plane Wave Generator + 2" Comp.B	Granite	Data, Table III
17	P-120 + 4" Comp. B.	Granite	Data, Table III
18	P-120 + 4" Comp. B.	Granite	Data, Table III
19	P-120 + 4" Comp. B.	Granite	Data, Table III
20	P-120 + 4" Comp. B.	Granite	Data, Table III
21	P-120 + 4" Comp. B.	Granite	Data, Table III

which was accentuated by the long leads required in the experiments. This problem was largely overcome by modifying the recording system and the gage design to minimize common-mode piezoelectric pickup.

A total of six experiments were conducted in Sioux quartzite with a maximum stress-wave propagation-distance of 4 inches. When an attempt was made to machine larger rock slabs from a block of quartzite, we found that internal cracks were spaced close enough to prevent machining even 1-foot-square slabs. These cracks were not at all apparent from visual inspection of the outside of the rough block. Therefore, we substituted charcoal black granite supplied by the Cold Spring Granite Company in Cold Spring, Minnesota.

The eleven experiments in granite yielded the most complete records. Except for one preliminary test shot, each experiment included five manganin stress gages. The development of the precursor was observed at 1-inch intervals to a propagation distance of 6 inches. The data indicate that time-dependent phenomena are not significant at this scale. The main phenomenon observed is the separation of the precursor from the main wave with increasing travel distance. The differences in precursor amplitude and waveform with increasing travel distance are not great and are attributed to experimental scatter caused primarily by large grain size and heterogeneous composition of the rock at the scale of the gage elements.

Seven experiments with wet and dry open cracks in granite showed very interesting results. The precursor, which is separated from the main wave by the time the crack is encountered, is, in effect, pushed back into the main wave. With further travel, the precursor once again begins to separate. Computer runs using SRI-PUFF were made and compared with the experimental records. The latter have wider variations in waveform and time separation than the computed profiles. The results suggest that in the field a crack volume of a percent or so may greatly change the precursor structure of a shock wave.

by insulating them between thin (about 0.003-inch) layers of Epon.* The plate-impact loading used was expected to produce a flat-topped pulse, but the waveforms showed stress decay immediately behind an early peak. Further experiments would be necessary to verify that a material property of the rock was being observed.

II EXPERIMENTAL RESULTS

A. Sioux Quartzite

Sioux quartzite was initially chosen to be the main rock used in the program. It is monomineralic (~ 99% quartz) with grains averaging about 0.1 mm in diameter (Ahrens and Gregson, 1964). For our specimens, the density averaged 2.624 ± 0.003 g/cm^3. For eight specimens, the ultrasonic velocity was 5.30 ± 0.05 km/sec, but for the ninth specimen, the velocity averaged 4.33 km/sec. Six experiments were completed before it was decided that the rock was not suitable for the size of experiments contemplated. Internal cracks limited the size of machined specimens that could be obtained.

Three experiments involved machined slabs of dry Sioux quartzite explosively loaded with P-120 plane-wave lenses and 4-inch-thick pads of TNT. In the first of these shots, timing from ionization gages at the explosive-rock interface did not work, so no records were obtained. In the second shot, timing was by electronic delay from the firing pulse. The stress gages used on the first two shots had sensitive elements 0.625-inch long made of flattened manganin wire 0.003-inch thick. The four leads on each gage were of 0.001-inch copper foil cut 0.063-inch wide. The records obtained on the second shot had so much noise pickup from the piezoelectric quartz grains along the 6- to 8-inch-long foil leads that the records could not be interpreted.

Two technique shots were designed to investigate the cause of the noise, each using two stress gages sandwiched between 4 x 4 x 1/2-inch slabs of Sioux quartzite. Explosive loading was by a P-40 plane-wave lens.

* Epon(R) adhesive 911F, Shell Chemical Company.

of 0.002-inch copper wire, flattened to about 0.0008 inch thick by 0.004 inch wide, instead of the copper foil used previously. Even with these narrower and shorter leads, pickup from the piezoelectric effect in the quartzite was still too high to permit precise readings from the records. However, we noted that pickup started at the time the shock hit the rock-explosive interface about 1/2 inch from the gages and did not grow much as the shock progressed past the gages. We concluded that the radiation from grains at distances of 1/2 inch and greater was more important than we had previously suspected, and therefore much of the electromagnetic pickup would be common mode.

On the next shot (No. 4), one gage used leads emerging from the side as in the first shot, while the other gage used wire leads emerging through holes drilled in the quartzite slab away from the explosive. A Tektronix Type G differential preamp was used on the leads of the gage emerging from the side of the shot. Pickup was reduced by about a factor of 5, thus giving acceptable data. The gage with leads emerging from the back of the shot showed little pickup until the wave progressed past the gage, at which point the record became unacceptably noisy. Leads emerging from the back of the shot through drilled holes are both more expensive to install and more likely to interfere with the wave propagation process. We will use them only when we need a long time response, since they generally do not break as quickly as gages contained completely in a crack between slabs.

Shot 5, on 12 x 12-inch slabs of Sioux quartzite (Fig. 1), used gages with 1/4-inch-long sensitive elements made of flattened 0.002-inch manganin wire. All leads were of flattened 0.002-inch copper wire emerging from the corners of the cracks. The voltage leads were laid as close together as possible (about 1 mm) to further improve common mode rejection of piezoelectric pickup. The stress wave record from gage No. 1 is shown in Fig. 2.

The transit times between the gages at 2 inches and 4 inches were 9.3 μsec for the precursors and 9.9 μsec for the main wave. Average

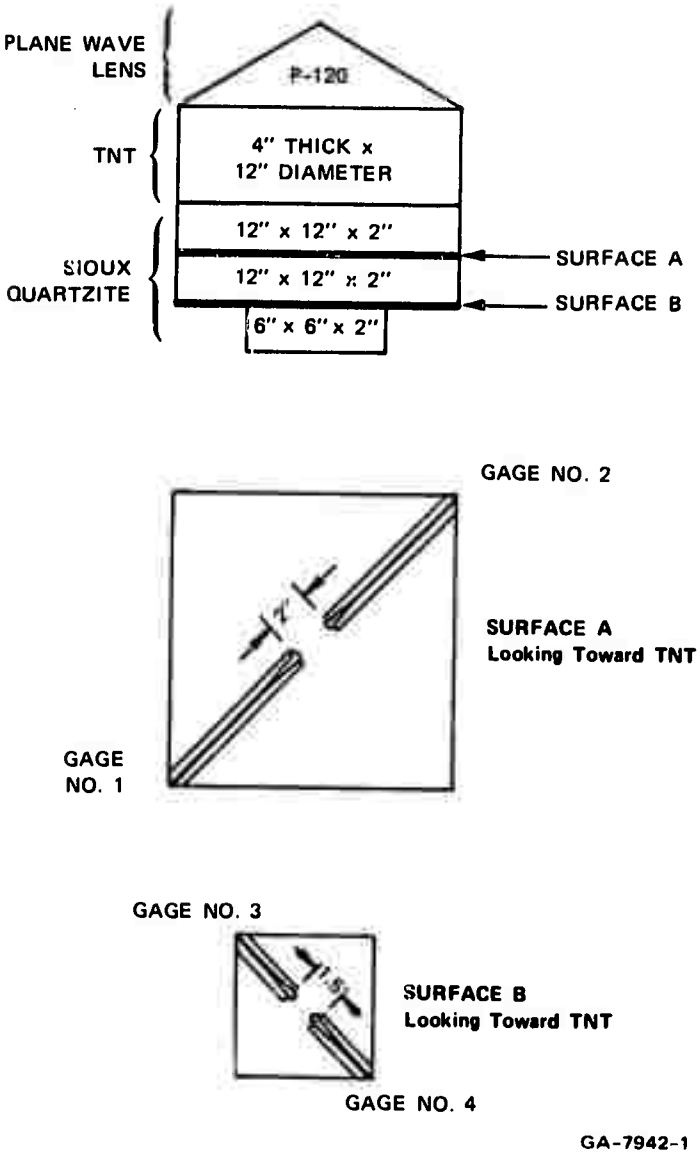

FIGURE 1 GAGE ARRANGEMENT FOR SHOT NO. 5

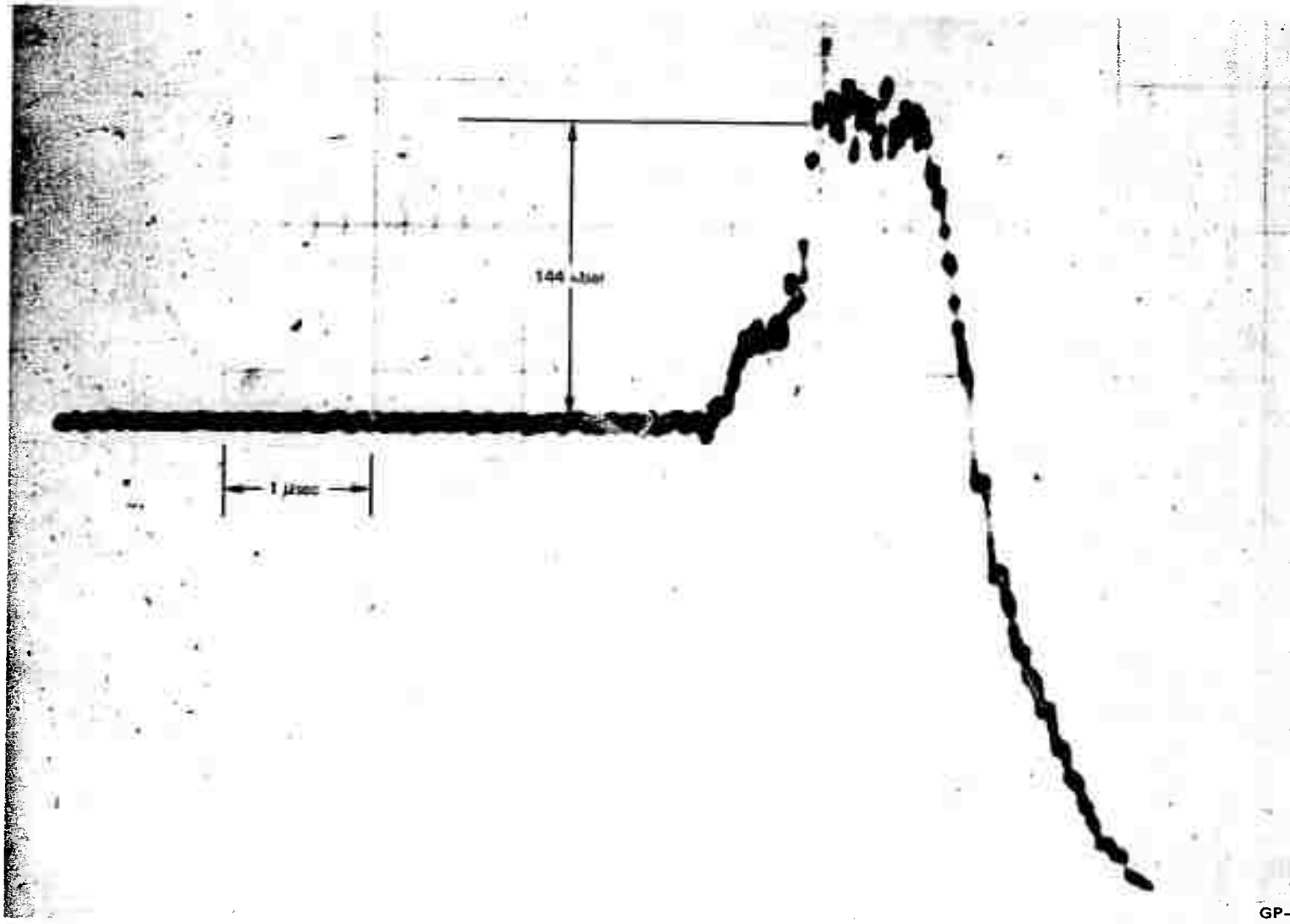

FIGURE 2 STRESS WAVE IN SIOUX QUARTZITE, GAGE NO. 1, SHOT NO. 5

slab before the shot but was over 5.22 km/sec on all other slabs. Unfortunately precursor transit times were not measurable for the other slabs. An unusually low ultrasonic velocity in one rock specimen is often caused by an unusually high number of microcracks. A high-amplitude precursor will close the cracks so that precursor velocities have less scatter than small amplitude ultrasonic waves.

Shot 6 was done to check whether the high-frequency noise on the records is produced by stress waves from formation and growth of cracks or by the piezoelectric effect. Two similar stress gages were built into the shot, one connected to our usual power supply and the other with no power supply attached. Both gages should have picked up piezoelectric noise equally, but only the gage with the current pulse would pick up noise from fracture-produced stress waves. Both gages picked up noise with equal RMS amplitude; hence it is concluded that the noise is piezoelectric.

The results of the Sioux quartzite experiments are given in Table II.

Table II

SIOUX QUARTZITE EXPERIMENTS

Shot No.	Gage No.	Rock Thickness (in.)	Precursor		Ramp		Main Wave	
			Rise Time (μsec)	Amplitude (kbar)	Duration (μsec)	Amplitude at Back (kbar)	Rise Time (μsec)	Amplitude (kbar)
2	2	2	-	-	-	-	(~0.37)	(149)
	3	4	(0.43)	(52.8	-	-	-	-
	4	4	(0.24)	(55.0)	-	-	-	-
3	1	0.501	0.16	38.5	0.28	56.3	0.19	102
	2	0.501	0.08	34.4	0.32	56.3	0.14	94.5
4	1	0.601	0.06	25.8	0.29	50.8	0.20	114.5
	2	0.601	0.15	33.8	0.29	(~65)	0.17	118
5	1	2	0.21	38.8	0.26	43.3	0.23	148.5
	2	2	0.18	33.3	0.35	50.4	0.26	141
	3	4	0.19	42.5	0.97	54.2	-	-
	4	4	0.14	35.7	-	-	-	-
8	1	0.61	0.22	42.0	0.17	51.8	0.30	116
Mean			0.15	35.9		51.9	0.21	
Standard Deviation			0.055	5.0		4.5	0.055	
Coefficient Variation			0.35	0.14		0.09	0.26	

Note: Results in parentheses are regarded as poor because the records were unusually noisy. These data were omitted from calculations of means and standard deviations.

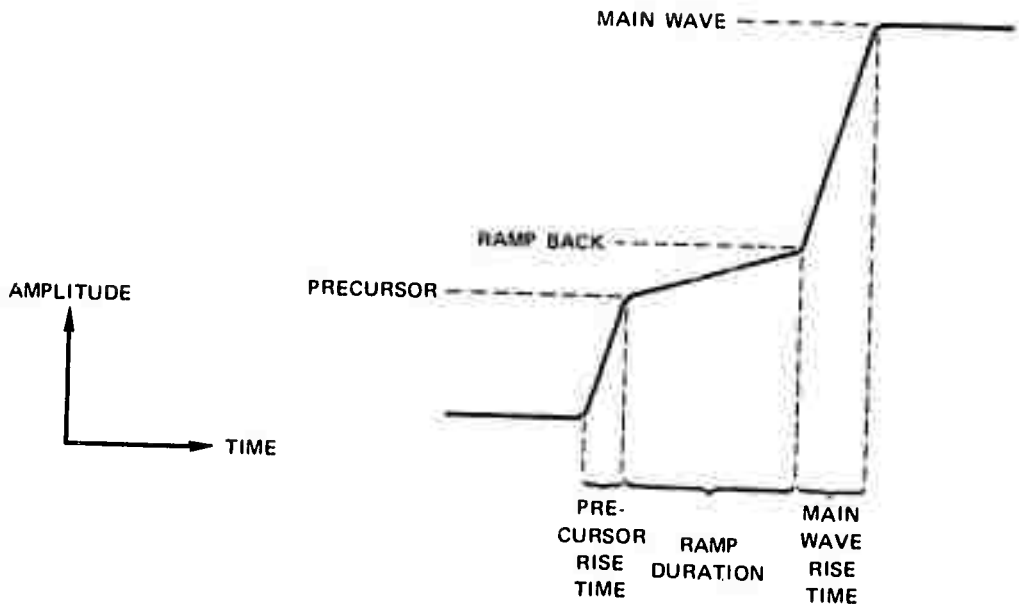

FIGURE 3 TERMINOLOGY USED TO DESCRIBE STRESS WAVE

Stress amplitude was calculated from the gage records by the linear relationship (Keough, 1968),

$$\sigma = \frac{\Delta R}{R} \times \frac{10^2}{0.29}$$

where σ is stress in kilobars, and $\frac{\Delta R}{R}$ is the ratio of the resistance change to the initial resistance of the manganin gage element. Since a constant current source was used and the resistance and resistance change of the active element is large compared with that of the leads in the speciman, $\frac{\Delta R}{R}$ is taken to be equal to the ratio of change in voltage to initial voltage as recorded by the oscilloscopes.

Shots 2 and 5 were loaded with a P-120 plane-wave lens plus a 4-inch-thick, 12-inch-diameter pad of TNT. The other three shots were loaded with P-40 plane-wave lenses only. Precursor rise time and amplitude, amplitude at the back of the ramp, and main wave rise time showed no

We conclude that the only nonsteady-state phenomenon observed was the increase in ramp length with rock thickness caused by the higher velocity of the precursor. Table II gives the means and standard deviations for rise times of the precursor and main wave and for amplitudes for the precursor at the front of the ramp and at the back of the ramp. Note that rise times are similar for the precursor and main wave. A measure of scatter of the data is given by dividing the standard deviation by the mean to obtain the coefficient of variation. This coefficient is smaller for main wave rise time than for that of the precursor. The coefficient of variation is also smaller for amplitude at the back of the ramp than for amplitude of the precursor at the front of the ramp. We conclude that details of the front edge of the precursor are more sensitive to rock inhomogeneities than details connected with the rise of the plane-wave from the back of the precursor.

B. Granite

Charcoal black granite supplied by the Cold Spring Granite Company of Cold Spring, Minnesota, was substituted for Sioux quartzite when the latter proved to be unsuitable for machining into large, uniform slabs. Our granite was quarried from the same site as that currently being used by Dr. Madan Singh of IITRI in a project involving triaxial testing of very large samples. The rock is massive with no noticeable preferred orientation of grains or texture. Most grains are between 1 and 5 mm in diameter. A few larger, denser, fine-grained inclusions are present. These showed up well in X rays of 1- and 2-inch-thick slabs, allowing selection of only the more uniform slabs for the construction of the shots. Except for the very large specimens, which could not be handled easily, all specimens were routinely checked for density, ultrasonic compressional velocity, and X-ray uniformity. Scatter within a specimen and from specimen to specimen was relatively small. Average density measured was 2.719 ± 0.003 g/cm^3, and average compressional velocity measured was 5.41 ± 0.12 km/sec.

A total of eleven experiments were conducted in the charcoal black granite. One was a simple test shot to evaluate piezoelectric noise and

experiments, each with five manganin stress gages. In Shots 12 and 13 the stress-time profile was recorded at 1-inch intervals in 6-inch-thick specimens. In Shots 14, 18, 20, and 21 the effect of a water-filled inclined crack was recorded. In Shots 15, 17, and 19 the crack was open and dry. In Shot 16 gages were placed at 2-inch intervals in a 12-inch thick specimen. A summary of results is given in Table III.

Shots 12 and 13 were very similar except for the manner in which the gages were inserted into the rock assembly (Fig. 4). In Shot 12, the rock was cut and machined into slabs 1-inch thick and more than 12 inches across all diameters. Six of these slabs were stacked to assemble the shot, with a manganin wire gage at each interface. The leads were brought out the largest dimension to the sides. The shot was fired with a P-120 plane-wave lens and a 4-inch by 12-inch diameter cylinder of Composition B high explosive.

In shot 13 a quarter-round, 6-inches thick and more than 12 inches across all diameters, was machined flat on one end where the explosive was to be placed. A 2-1/2-inch diameter core was drilled out of the center, perpendicular to the machined surface. One-inch-thick discs of granite were then machined to fit snugly (< 0.010-inch glue line across the diameter) back into the hole. Five manganin wire stress gages were fitted into the core, one at the center of each disc interface. Copper leads were used from the manganin element to the circumference of the core. Leads were brought out to the back of the shot in narrow slots cut into the circumference of the core and filled with dental amalgam.

Good quality records were obtained from all gages for shots 12 and 13 (Table III and Fig. 5). The two shots were very similar in showing the rate of precursor development. The precursor is slower to separate clearly from the main wave in granite than it is in quartzite (Fig. 6) probably because of the larger grain size and the more varied mineralogy. The scatter in precursor amplitude appears to be random, caused by large grain size and heterogeneous composition of the rock at the scale of the gage elements. The precursor amplitude and waveform does not seem to be affected significantly by time or distance of propagation. This is an important result because of the question of the validity of small-scale laboratory experiments to determine rock properties that are required for in situ problems.

Table III

GRANITE EXPERIMENTS

Gage	Thickness (mm)	Precursor		Ramp		Main Wave	
		Rise Time (μsec)	Ampl. (kbar)	Rise Time (μsec)	Ampl. at Back (kbar)	Rise Time (μsec)	Ampl. (kbar)
SHOT 12							
1	26.96	0.28	26	0.12	36	0.30	150
2	53.71	0.40	25	0.26	46	0.26	173
3	60.70	0.67	38	0.36	53	0.37	144
4	106.57	0.61	27	0.93	61	0.36	152
5	133.51	0.67	33	1.15	56	0.40	140
SHOT 13							
1	25.42	0.37	30	0.0	30	0.20	181
2	51.43	0.40	22	0.40	37	0.16	116
3	76.93	0.76	41	0.33	60	0.26	156
4	102.39	0.50	27	0.60	50	0.37	183
5	127.91	0.53	25	1.07	50	0.63	158
SHOT 14							
1	25.55	0.2	26	--	--	0.8	181
2	78.05	0.56	26	0.46	45	0.62	173
3	78.05	0.62	30	0.20	49	0.26	151
4	79.05	--	--	0.58	42	0.25	141
5	104.06	0.57	32	0.47	52	0.36	154
SHOT 15							
1	26.34	0.26	32	--	--	0.60	173
2	78.31	0.56	33	0.54	60	0.23	156
3	78.31	--	--	0.47	75	0.06	140
4	76.31	--	--	0.37	55	0.20	163
5	104.37	0.43	31	0.47	47	0.23	136
SHOT 16							
1	49.65	Gage failed before HEL was reached.					
2	101.96	0.4	26	1.3	42	--	--
3	152.34	0.62	20	2.15	40	0.62	140
4	203.70	No records obtained					
5	254.78	No records obtained					
SHOT 17							
1	51.99	--	--	0.65	50	0.20	178
2	76.05	0.28	30	0.37	56	0.23	168
3	78.05	0.50	33	0.31	52	0.26	154
4	104.72	0.41	25	0.68	50	0.45	132
5	104.72	0.39	31	0.64	57	0.52	176
SHOT 18							
1	51.66	0.45	30	0.34	50	0.30	203
2	78.12	--	--	1.14	67	0.24	182
3	78.12	--	--	1.08	63	1.19	188
4	103.24	0.62	31	0.72	54	0.38	152
5	103.24	0.60	35	0.60	54	0.39	186
SHOT 19							
1	26.95	--	--	0.26	75	0.20	(280)
2	79.40	--	--	0.98	63	0.32	197
3	79.40	--	--	1.00	50	0.24	185
4	106.65	0.60	29	0.82	45	0.42	153
5	106.65	0.53	34	0.75	45	0.35	170
SHOT 20							
1	26.44	--	--	0.41	63	0.14	200
2	76.89	0.82	35	0.22	42	0.21	178
3	78.89	0.63	42	0.30	55	0.24	175
4	105.	0.44	22	0.91	60	0.19	172
5	105.	0.65	28	0.93	52	0.26	156
SHOT 21							
1	52.27	0.46	10	0.23	31	0.39	165
2	77.90	0.59	19	0.33	51	0.41	160
3	77.90	--	--	0.64	56	0.50	170
4	103.48	0.32	25	0.74	50	0.28	157
5	103.46	0.33	35	0.35	42	0.46	150

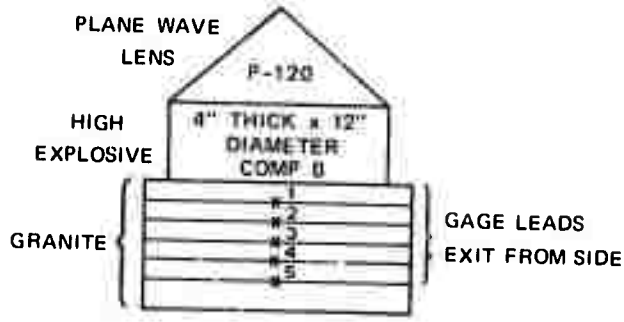

(a) SHOT NO. 12

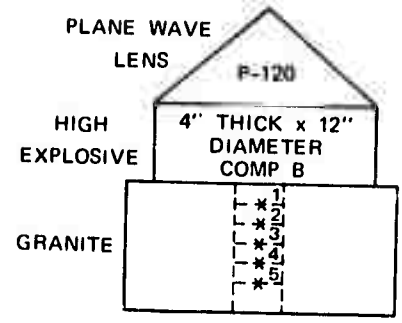

(b) SHOT NO. 13

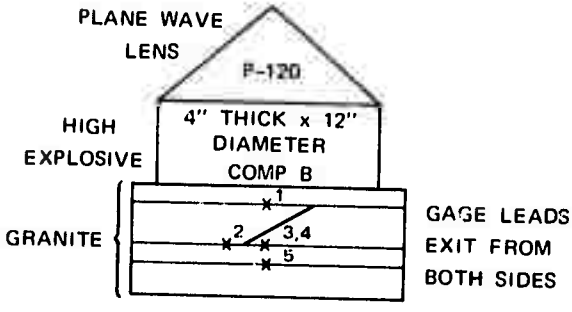

(c) SHOTS NO. 14 AND 15

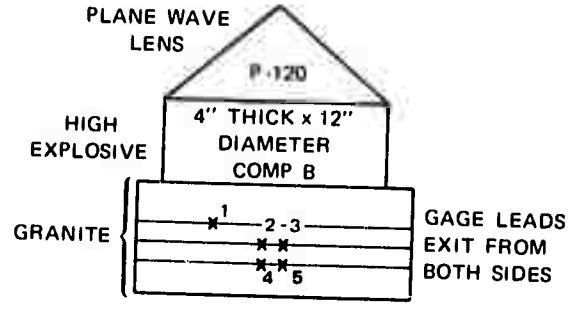

(d) SHOTS NO. 17, 18, AND 21

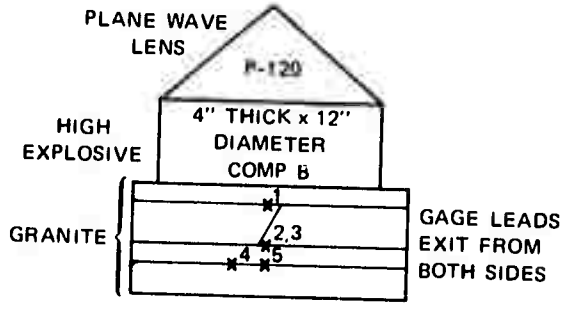

(e) SHOTS NO. 19 AND 20

GA-7942-5B

FIGURE 4 GAGE ARRANGEMENTS FOR GRANITE EXPERIMENTS. x^3 indicates gage location and number.

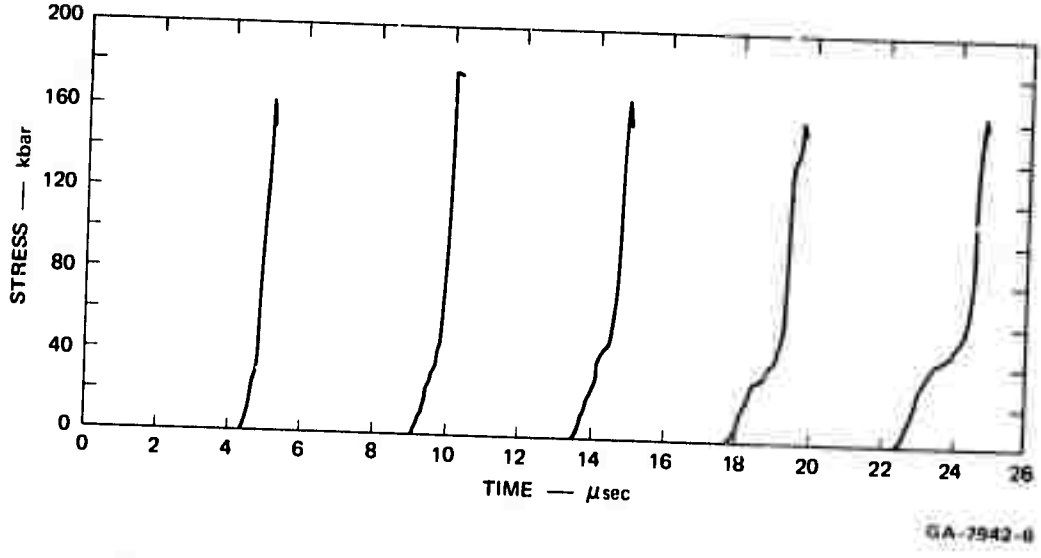

FIGURE 5 PRECURSOR DEVELOPMENT IN GRANITE. Gages at 1 inch intervals. Shot No. 12.

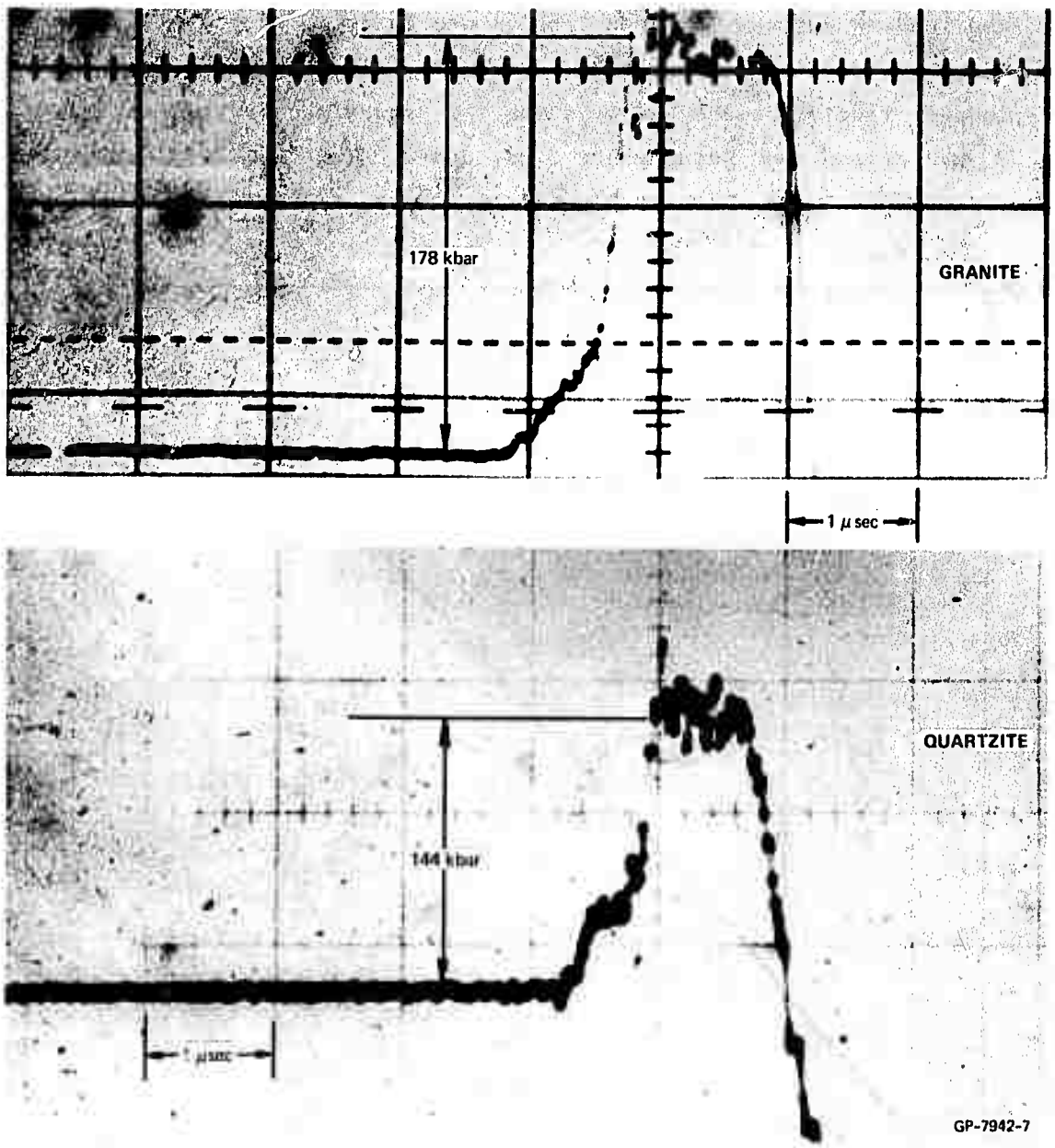

FIGURE 6 PRECURSOR IN GRANITE COMPARED WITH PRECURSOR IN QUARTZITE BOTH AT 2 INCH DEPTH. Shots 12 and 5.

Gage records in the granite experiments were good enough, in contrast to the more noisy quartzite records, to permit the use of Lagrangian analysis to derive the stress particle velocity and stress-volume loading curves. Figures 7 and 8 and Table IV show average loading curves obtained for the granite. The significance of time-dependent effects was checked by doing the analysis using, first, gages 1, 2, and 3, and then using gages 3, 4, and 5. The resulting curves were nearly identical, as shown in Fig. 8.

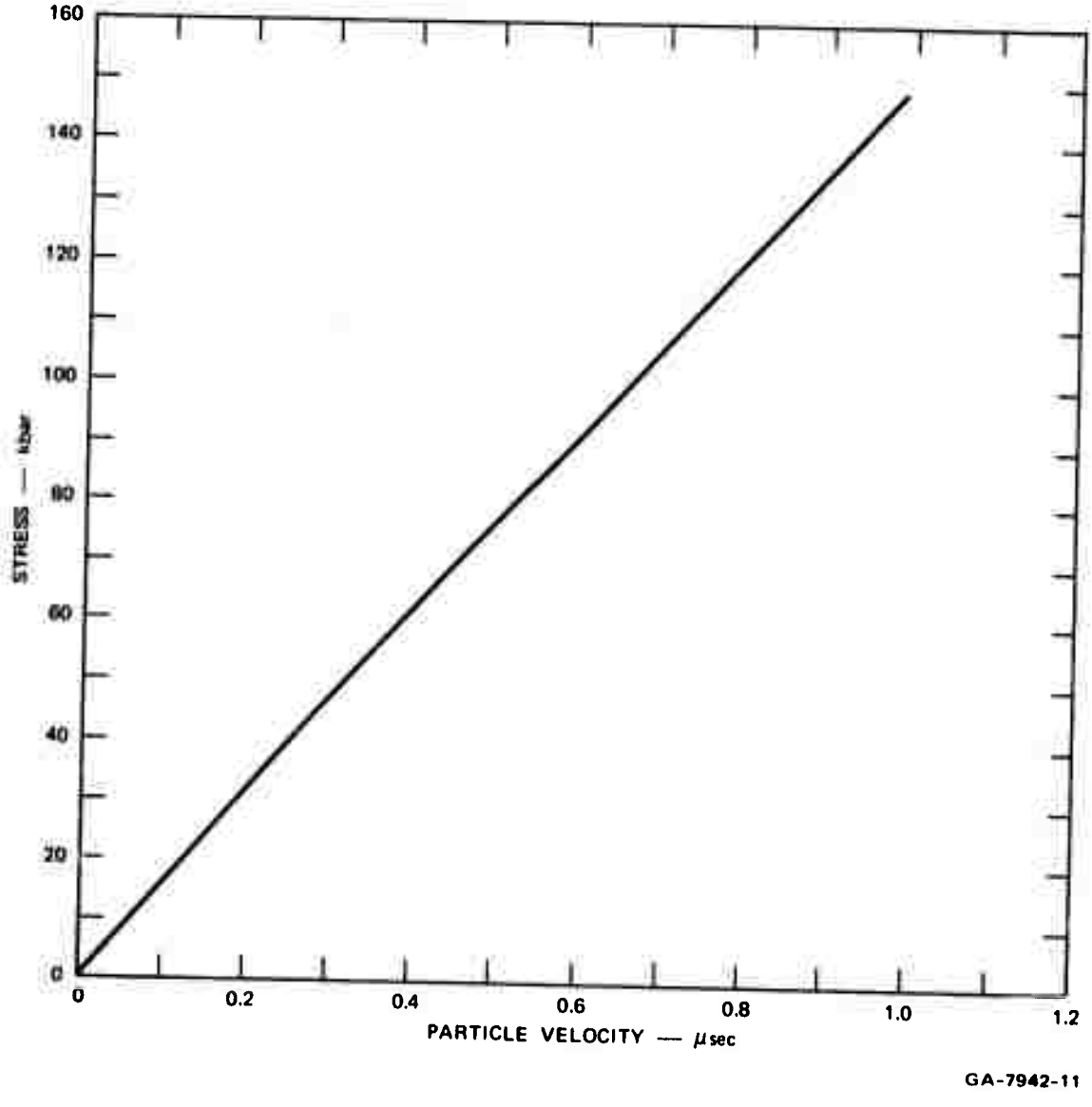

FIGURE 7 STRESS-PARTICLE VELOCITY LOADING CURVE FOR GRANITE. Obtained by Lagrangian analysis of Shot No. 12.

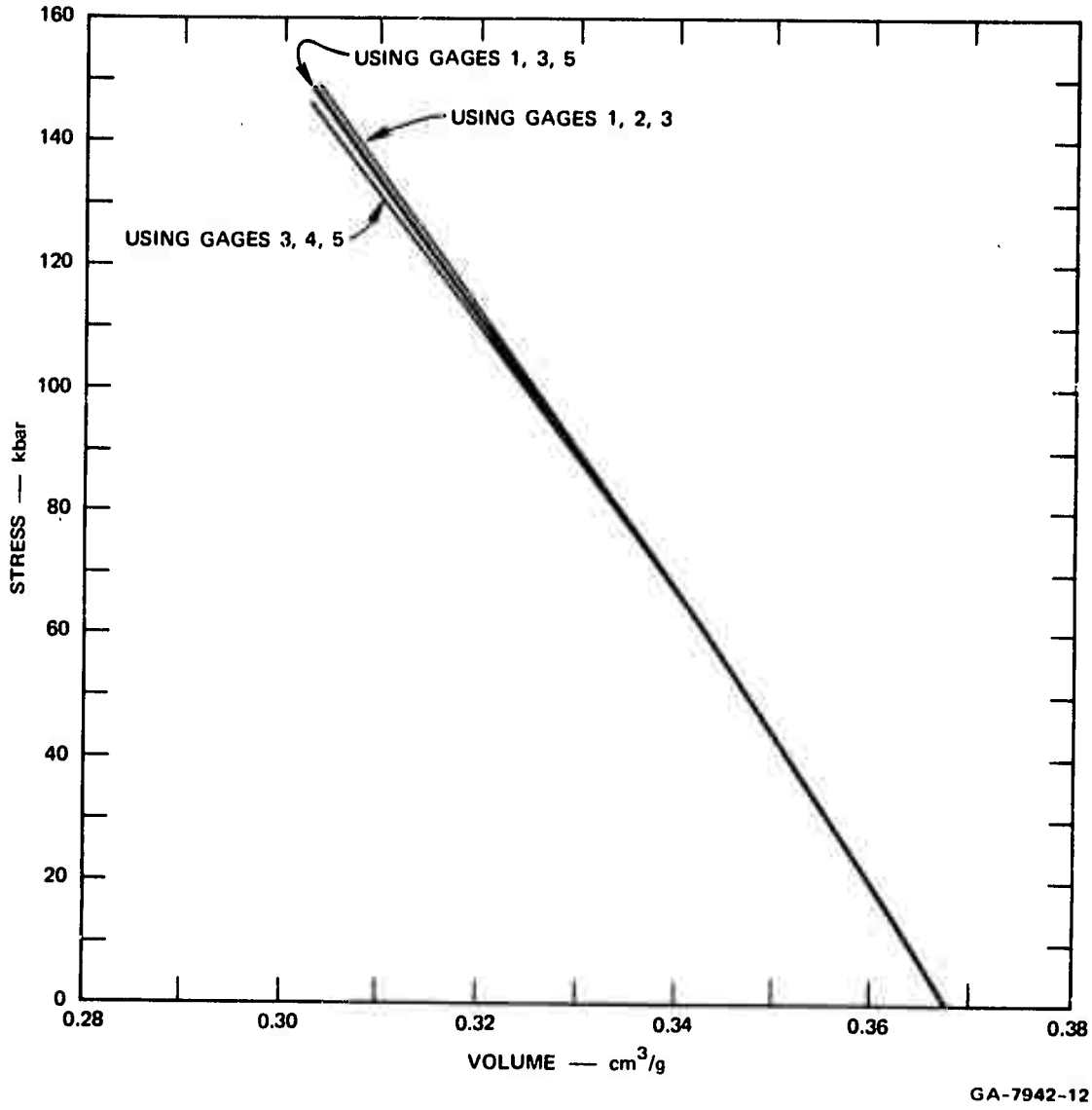

FIGURE 8 STRESS-VOLUME LOADING CURVES FOR GRANITE. Obtained by Lagrangian analysis of Shot No. 12.

Lagrangian analysis is described in general by Fowles and Williams (1970). In our present work we consider that stress is a function of particle velocity only, which simplifies the calculations. The fact that the loading curves derived from gages 1, 2, and 3 are nearly identical to those derived from gages 3, 4, and 5 indicates that this assumption is warranted. The computer program is given in detail by Murri and Smith (1970).

Table IV

LOADING CURVE FOR GRANITE, SHOT NO. 12, GAGES 1, 3, 5

Stress (kbar)	Particle Velocity (mm/μsec)	Volume (cm^3/g)	Local Sound Speed (mm/μsec)
0	0	0.3676	5.905
5	0.0312	0.3656	5.858
10	0.0624	0.3637	5.806
15	0.0938	0.3617	5.759
20	0.1253	0.3597	5.709
25	0.1568	0.3578	5.661
30	0.1884	0.3558	5.618
35	0.2202	0.3537	5.545
40	0.2523	0.3517	5.461
45	0.2849	0.3495	5.306
50	0.3180	0.3474	5.227
55	0.3513	0.3451	5.157
60	0.3848	0.3429	5.110
65	0.4184	0.3406	5.065
70	0.4521	0.3384	5.022
75	0.4858	0.3361	4.987
80	0.5195	0.3338	4.950
85	0.5532	0.3315	4.915
90	0.5869	0.3293	4.882
95	0.6206	0.3270	4.850
100	0.6544	0.3247	4.818
105	0.6880	0.3224	4.785
110	0.7217	0.3202	4.753
115	0.7554	0.3179	4.721
120	0.7891	0.3156	4.689
125	0.8227	0.3134	4.657
130	0.8564	0.3111	4.622
135	0.8900	0.3088	4.587
140	0.9237	0.3066	4.550
145	0.9574	0.3043	4.513
148	0.9776	0.3030	4.491

In the calculations, particle velocity is first obtained by

$$u_i = u_{i-1} + \frac{1}{\rho_o} \int \frac{d\sigma}{dh/dt}$$

with dh/dt estimated from the gage data. Here u_i is the particle velocity at the i^{th} point (initially u_{i-1} is zero for compression calculations), ρ_o is the initial density, h is the Lagrangian distance coordinate specifying the positions of the gages, σ is the stress, and t is the time. Next, the volume is computed by integrating the equation

$$V_i = V_{i-1} - \frac{1}{\rho_o^2} \int \frac{d\sigma}{(dh/dt)^2}$$

where V_i is the volume of the i^{th} point (initially V_{i-1} is the zero stress volume, $\frac{1}{\rho_o}$).

The local sound speed is then calculated from the equation

$$C_i = \left| \rho_o \; V_i \; \frac{dh}{dt} \right|$$

where C_i is the sound speed of the i^{th} point.

Shots 14 and 15 were designed to record the effects of open cracks, dry and water-filled, on the stress profile. In both experiments a 30° angle cut was made in a 2-inch-thick slab of granite. The cut was machined and held open 0.005 inch. In Shot 14 the crack was filled with water under vacuum and sealed; in Shot 15 the crack was left dry. The assembly is shown in Fig. 4c. The explosive chain, a P-120 and a 4-inch pad of Composition B, is in contact with a 1-inch slab of granite, which is followed in turn by the 2-inch slab with the 30° cut, a 1-inch slab, and a covering 1-1/2-inch slab. Stress gages are located between slabs of granite. Beneath the 2-inch slab, two gages are positioned under the open cut and one gage on the other side of the cut.

Gage records of the two experiments are shown in Figs. 9 and 10. In both experiments, the records from the gages beneath the cuts show an erasing of the precursor as can be seen by comparing records from

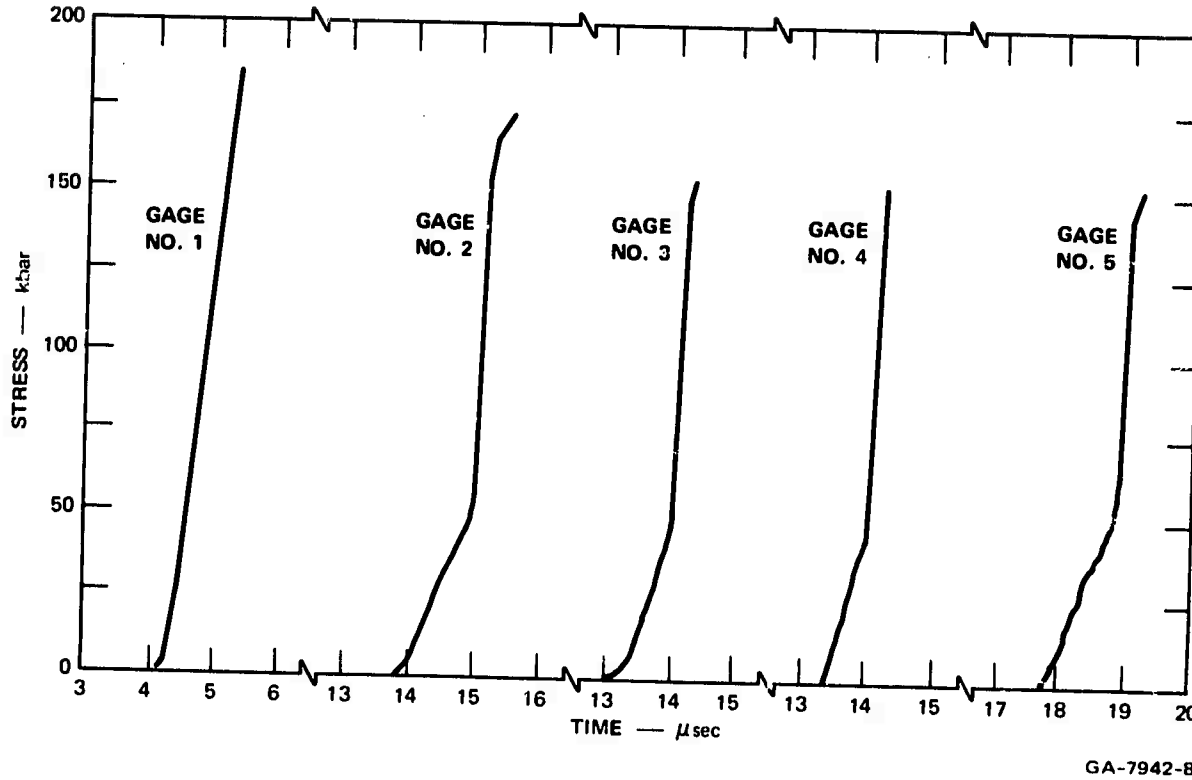

FIGURE 9 STRESS-TIME RECORDS FROM SHOT 14. Gages 3 and 4 are below water-filled crack. Gage 2 is at same plane but not below crack.

gage 2 with those from gages 3 and 4. The erasing is more complete in the case of the dry crack (Fig. 10).

Computer runs using SRI PUFF (Seaman, 1970) have been made, treating the crack as a layer normal to the direction of stress wave propagation. An approximation to the experimentally measured stress-time pulse was allowed to propagate across the crack to the recording position below the crack. The three cases treated, no crack, water-filled crack, and dry crack, are shown in Fig. 11 along with experimentally recorded profiles. The curve from Shot 15 in Fig. 11b has been adjusted in arrival time to agree with the curves from Shot 14. Several important observations can be made: (1) The experimental profiles have more variations in waveform and time separation than the computed profiles. This may be partly experimental scatter, but study of Figs. 9 and 10 shows that

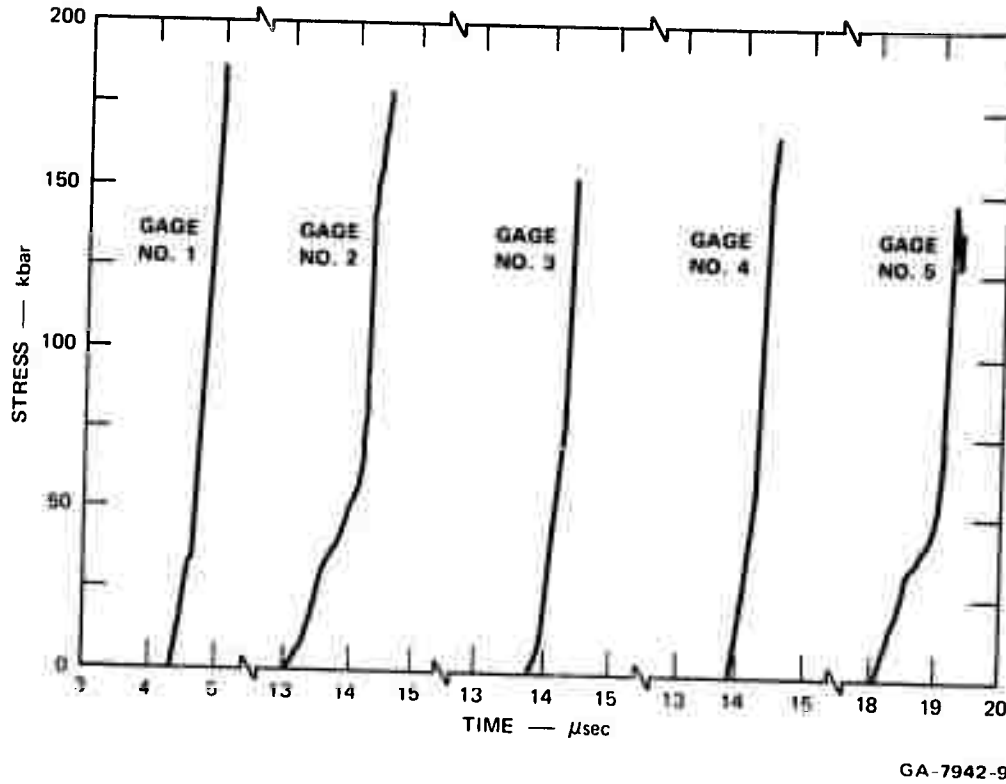

FIGURE 10 STRESS-TIME RECORDS FROM SHOT 15. Gages 3 and 4 are below dry crack. Gage 2 is at same plane but not below crack.

gage records 3 and 4 from below the crack are, in each case, very similar. (2) The water-filled crack profile, as computed, lies closer to the solid profile than to the dry crack profile. The experimental records show the reverse. However, later experiments, discussed below, are more in agreement with the computation. (3) The computed slopes are not as steep as the recorded slopes. This is a fault of the artificial viscosity computation and could be improved with longer runs.

Shot 16 was the largest experiment of the program. It was similar in design to Shot 13 in that gages were placed between discs of rock in a cylindrical core that was inserted into a machined hole in the center of the large specimen. Five gages were used at intervals of 2 inches. A mouse-trap plane-wave generator (Duvall and Fowles, 1963) with a geodesic line wave initiator (Erkman, 1959) was used to detonate a

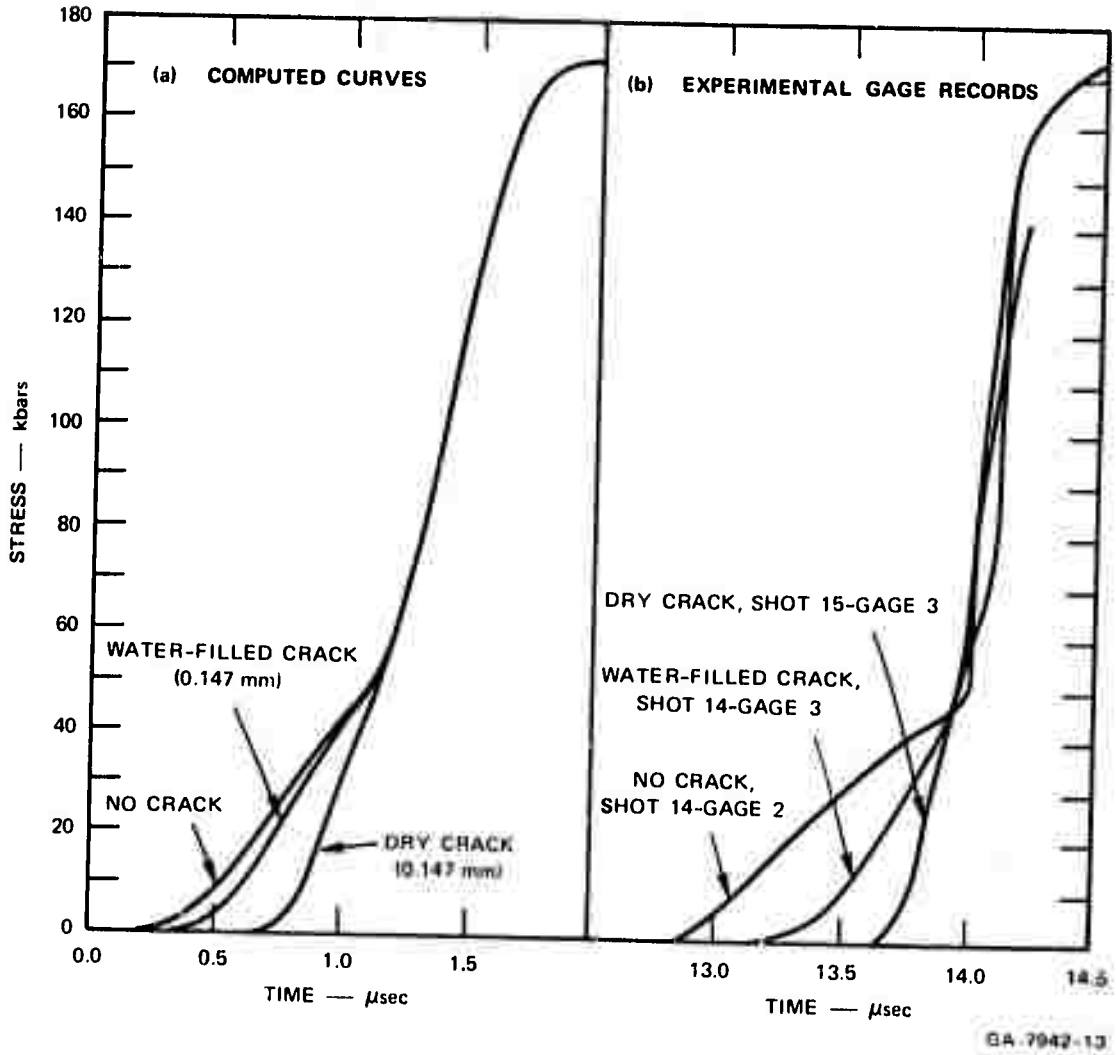

FIGURE 11 COMPUTED AND EXPERIMENTAL GAGE RECORDS COMPARING EFFECTS OF WATER-FILLED AND DRY CRACKS IN GRANITE

24 x 24 x 2 inch slab of Composition B high explosive in contact with the rock surface. An experiment was conducted in an attempt to sensitize nitromethane so that it could be used as the explosive to be initiated by the mouse-trap arrangement in our intended experiments on 2 x 2 ft rock slabs. With a mouse-trap arrangement we attempted to initiate plain nitromethane, nitromethane with 1% triethylamine added, plain

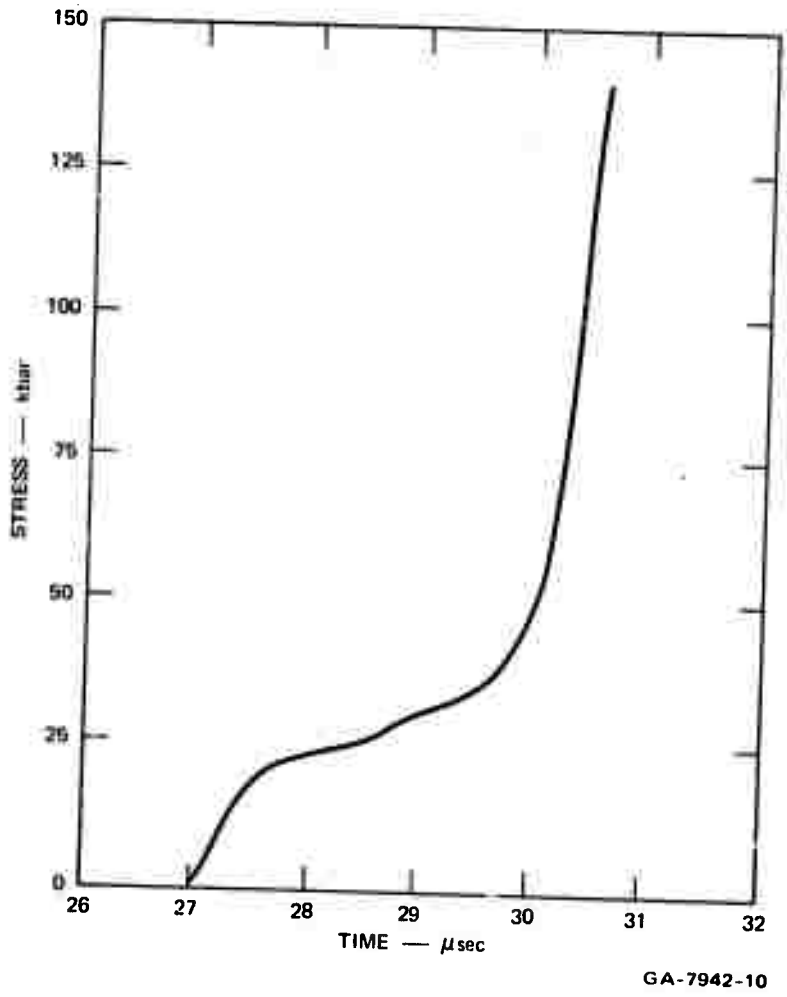

FIGURE 12 PRECURSOR IN GRANITE AT 6 INCHES FROM EXPLOSIVE-GRANITE INTERFACE. Shot No. 16.

nitromethane with floating micro balloons, and nitromethane with 1% triethylamine plus floating micro balloons. None of the arrangements gave a satisfactory detonation from the mouse-trap loading. Therefore, we decided to use the more expensive and less uniform machined Composition B slabs for the explosive in the large shots.

Results for Shot 16 are summarized in Table III. Gage 1 shorted out early in the precursor rise, giving only time-of-arrival data. Gage 2 recorded the precursor development and failed during the arrival of the main shock. Gage 3 shows a complete record of the shock compression

(Fig. 12). Unfortunately, a time delay generator malfunctioned causing the loss of records from gages 4 and 5.

Shots 17 and 18 were identical in construction except that the horizontal 0.006-inch open crack was dry in Shot 17 and filled with water in Shot 18. Gage records are shown in Fig. 13 and 14. The records for gages 2 and 3, located 1 inch beyond the crack, show that the dry crack in Shot 17 causes the precursor to have a steep rise to about 30 kbar, whereas in Shot 18 the precursor rises more slowly and evenly to about 60 kbar. In Shot 17 the rise from 0 to 50 kbar takes about 0.7 μsec; in Shot 18 it takes 1 μsec. In the first case the crack has to be closed before energy is transmitted beyond the crack. In the second some stress wave energy is transmitted directly through the water. A series of reverberations permits the rest of the energy to be transmitted. The result is seen as a slower rise time from zero stress at gages 2 and 3. Little difference is seen by the time the stress wave reaches gages 4 and 5. Local inhomogeneities obscure the finer details of the waveform.

In Shots 19 and 20 the 0.006-inch open crack was inclined at 60^{o} to the horizontal. The cracks were dry in Shot 19 and filled with water in Shot 20. The gage records for the two shots, shown in Figs. 15 and 16, are not significantly different. Presumably, the inclination of the crack causes the effect on the precursor to be spread out over time and over the area of the gage, making the differences between the wet and dry cracks less obvious.

Shot 21 was identical to Shot 18, with a water-filled horizontal crack, except that in Shot 21 the crack width was increased to 0.024 inch from the 0.006 inch of No. 18. The records are shown in Fig. 17. In general they are similar to those of Shot 18 (Fig. 14). However, a pronounced effect on the shape of the precursor can be seen in Fig. 18, which compares gage records at similar positions in Shots 12 and 13, 17, 18, and 21. In each case the average of two gage records is plotted with times adjusted for simultaneous arrival of the main wave. The average

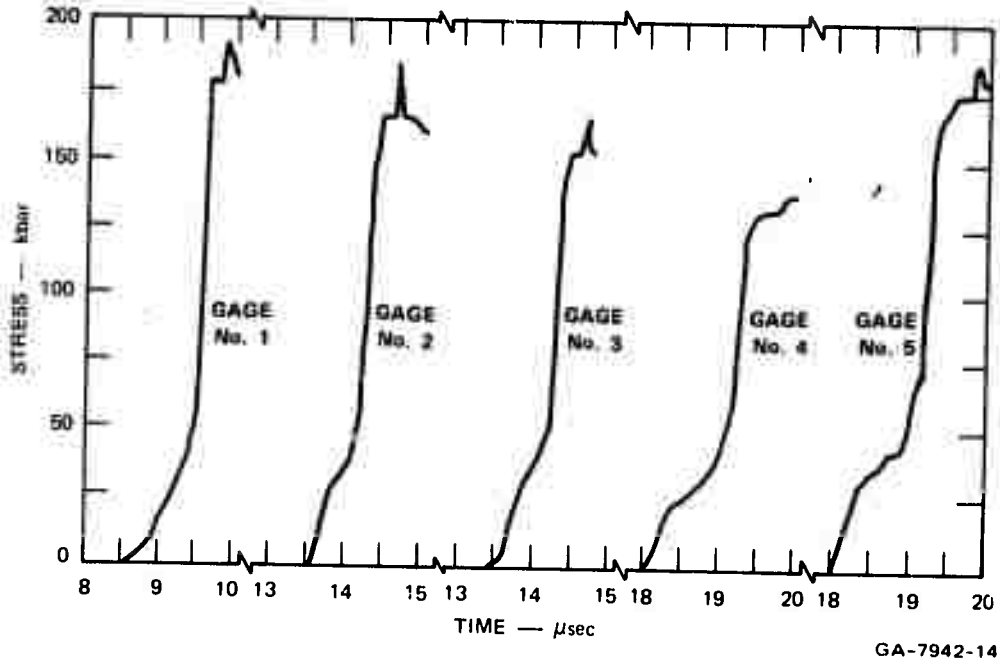

FIGURE 13 STRESS-TIME RECORDS FROM SHOT 17

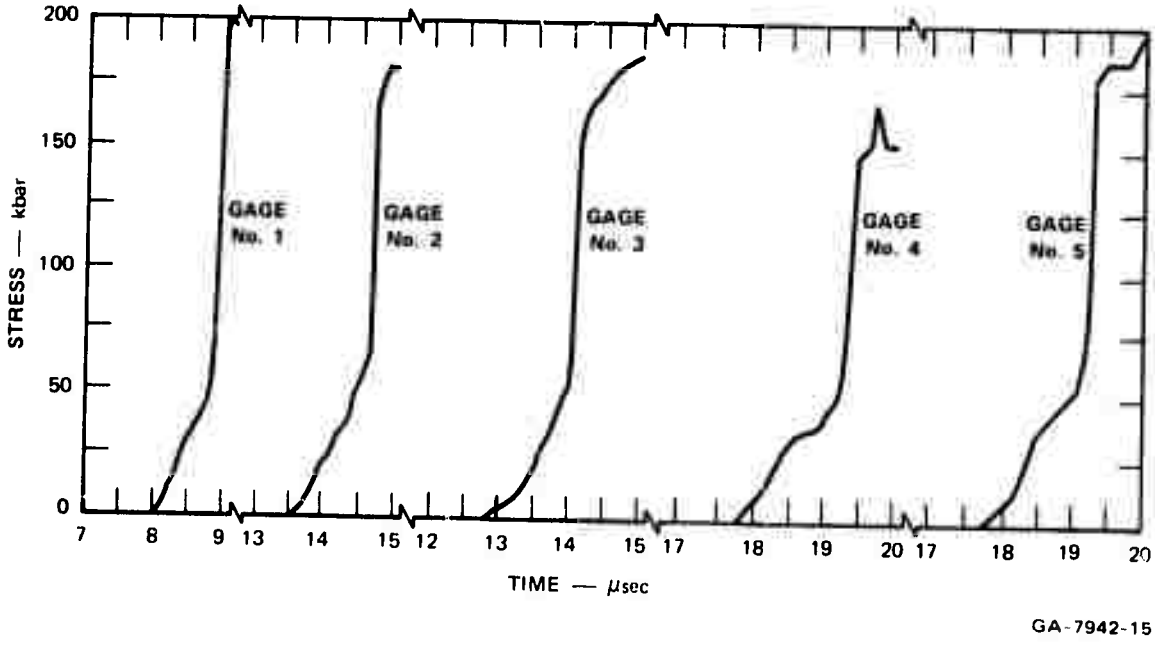

FIGURE 14 STRESS-TIME RECORDS FROM SHOT 18

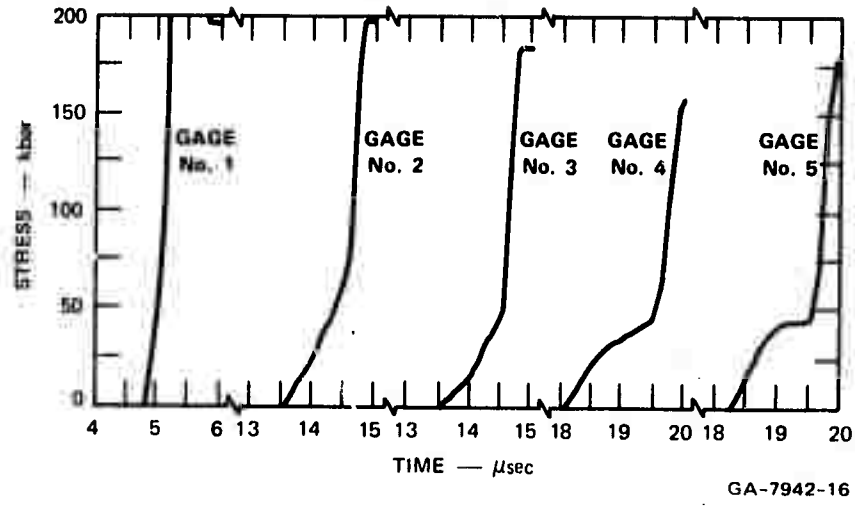

FIGURE 15 STRESS-TIME RECORDS FROM SHOT 19

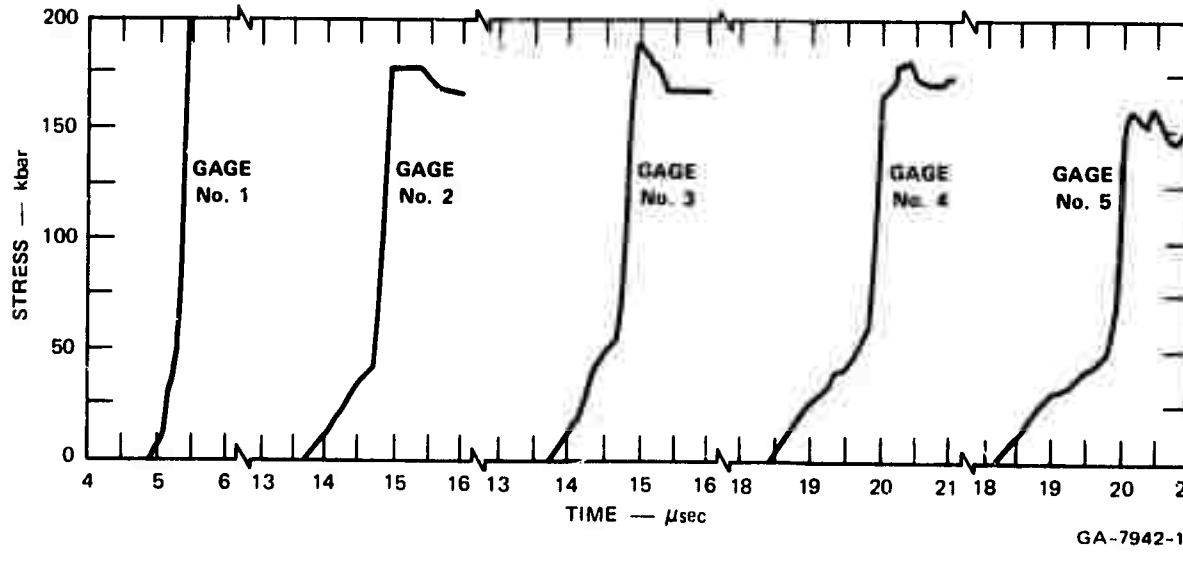

FIGURE 16 STRESS-TIME RECORDS FROM SHOT 20

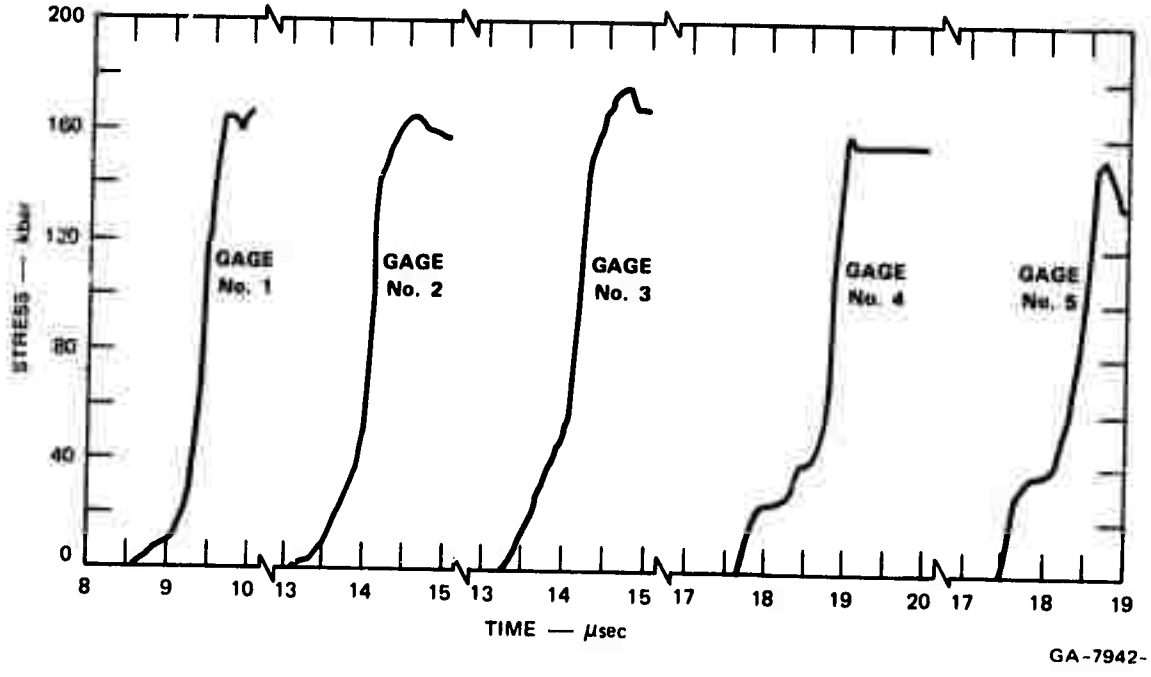

FIGURE 17 STRESS-TIME RECORDS FROM SHOT 21

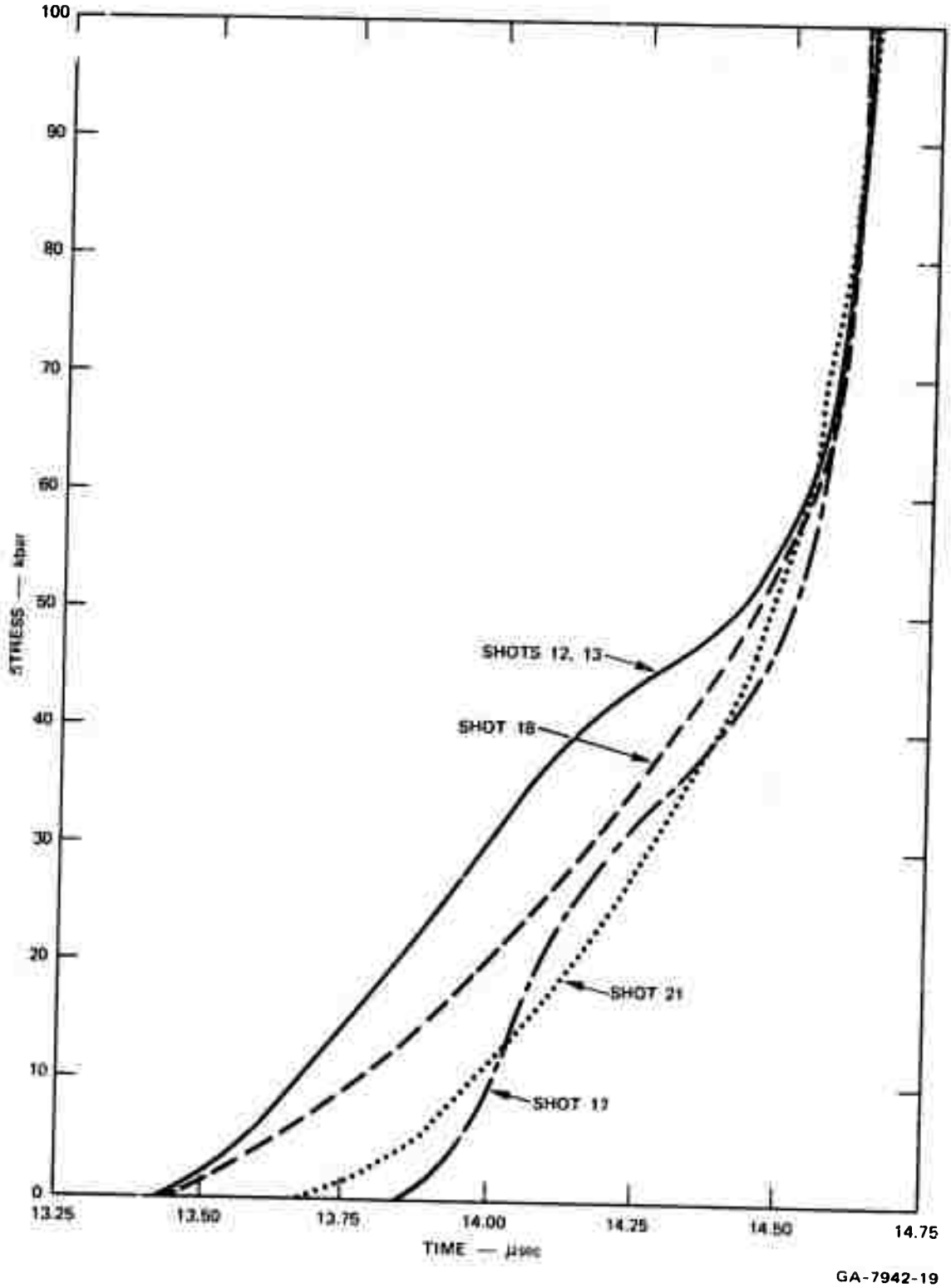

FIGURE 18 EXPERIMENTAL RECORDS OF EFFECTS OF CRACKS ON STRUCTURE OF PRECURSOR IN GRANITE

of gages 2 and 3 for Shot 18 shows much less precursor structure but just as much overall risetime. The average of gages 2 and 3 in Shot 21 shows almost no precursor structure and less rise time. The similar record for Shot 17 with the dry crack is shown for comparison. As noted above, the precursor structure remains, but the risetime is reduced significantly. Since gages 2 and 3 are 1 inch from the crack, the crack itself, even in Shot 21, is only 2.4% of the distance from the crack to the gages. In Shot 18 the crack is only 0.6% of that distance. These results suggest that in the field a crack volume of a percent or so may greatly alter the precursor structure of a shock wave.

C. Coconino Sandstone

Coconino sandstone was chosen for use as the porous rock in the program. It is nearly monomineralic (97% quartz, 3% feldspar, with a weak silica cement). The grain size is 0.1 to 0.2 mm in diameter (Ahrens and Gregson, 1964). Our specimens had a porosity of about 20%. The ultrasonic sound velocity was 3.27 km/sec.

Four experiments were performed on Coconino sandstone, two with the rock dry and two with the rock saturated with water. The first two shots, one wet and one dry, were otherwise similar, consisting of two slabs of sandstone, approximately 8 x 10 x 1/2-inch thick, cut parallel to the bedding. Three gages were inserted in the crack between the two sandstone slabs, each gage in a different insulating material. The main purpose of these preliminary experiments was to check the effectiveness of glass, mica, and Epon* adhesive as insulating and armoring material to prevent shorting or breaking of in-material gages in the porous sandstone. An additional manganin gage was used on the back surface of each shot in a C-7 buffer.

* Epon (R), adhesive 911F, Shell Chemical Company.

The loading of each shot was by impact of a 1/2-inch aluminum flyer plate driven by a P-80 wave lens plus a 2-inch Baratol pad. The glass-insulated gages did not work in either shot; traces were too noisy to read. Mica and Epon insulation worked in both shots, although the Epon insulation gave a longer recording time. Mica-insulated gages indicated 114-kbar peak stress in the dry shot and 160-kbar in the wet shot. Epon-insulated gages indicated 128-kbar peak stress in the dry shot and 174-kbar in the wet shot. The gage in C-7 on the back surfaces gave a peak stress of 63 kbar in the dry shot and 82 kbar for the wet shot. An impedance match solution using the previously determined Hugoniot equations of state for Coconino sandstone (Gregson et al., 1963) and for C-7 (Keough, 1968) gave approximate peak stresses of 71 kbar at the back surface for the dry shot and 106 kbar for the wet shot. Waveforms at both the internal and back surface gages did not have flat tops as expected from plate impact but showed stress decay immediately behind an early peak. This waveform is characteristic of a shock being attenuated by and overtaken by rarefaction. This interpretation checks with the apparent attenuation between the in-material gages and the back surface gages, but the rarefaction from the back of the 1/2-inch aluminum flyer could not overtake the shot at 1/2-inch depth in the dry sandstone. Our only explanation at present is that a stress relaxation occurs after the plate impact on the dry sandstone. The internal gages in the wet sandstone did not record long enough to show whether significant stress decay occurred after the initial peaks. The C-7 gage on the back of the wet shot showed a decaying stress.

The next shots fired in Coconino sandstone, one dry and one water saturated, were similarly impacted with a 1/2-inch Al flyer plate driven by a P-80 plane wave lens and 2 inches of Baratol. Each shot was instrumented with manganin stress gages at the impact surface, and at nominal distances of 1/2, 1, 2, and 3 inches from the impact surface. Each gage was cemented between two sheets of Epon 0.003 inch thick. This gage-sandwich (total thickness about 0.007 inch) was then placed between slabs of sandstone. In the case of the water saturated shot, the slab faces

were coated with Homolite epoxy. The penetration of the epoxy into the sandstone was about 0.015 inch or about 2 grain diameters. The sandstone slabs were then saturated by allowing water to enter under vacuum from the ends of each slab. Unfortunately, in the water saturated shot, the gage leads were cut by the explosive chain, and measurements were not obtained. In the dry shot, all the stress gages functioned properly (see Fig. 19) except for the one on the impact surface. The impact surface gage was insulated with 0.002-inch of Kapton sheet,* but the gage shorted at the instant of impact. Stress amplitudes and rise times for the four successful gages are given in Table V. Average shock velocities between positions are also given.

The rarefaction from the back side of the flyer plate should catch the shock front at about the position of the third gage. The exact time of catch-up is uncertain because the rarefaction velocity in the compressed sandstone is not known. To estimate the time of catch-up, we assumed 7.0 mm/μsec, which is about twice the shock velocity. Our previous work on porous playa alluvium indicates that such a value is reasonable (Petersen et al., 1970).

III RECOMMENDATIONS

The four sandstone experiments were disappointing in that the few results obtained cannot be given a clear-cut interpretation. At some future date, a program to study stress wave propagation through thick specimens of porous rock would be desirable. This would necessarily be a larger effort with additional work in gage development and emplacement techniques to ensure useful results. With further development for use in explosive experiments, particle velocity gages (Petersen et al., 1970) may prove to be superior to stress gages for use in highly porous rocks.

---

* Kapton is similar to Mylar but stronger. Lawrence Livermore Laboratory has successfully used it to insulate manganin gages in aluminum at several hundred kbar.

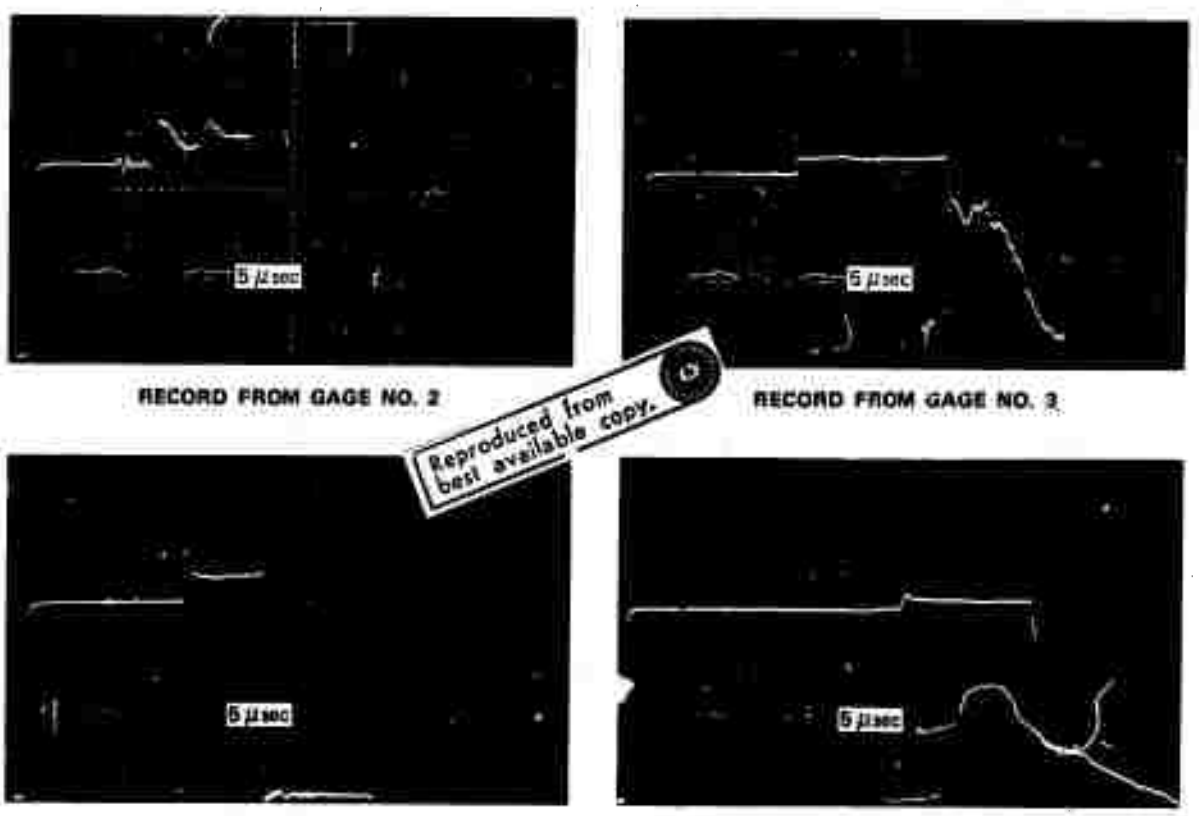

RECORD FROM GAGE NO. 2

RECORD FROM GAGE NO. 3

RECORD FROM GAGE NO. 4

RECORD FROM GAGE NO. 5

GP-7942-4

FIGURE 19 GAGE RECORDS FOR DRY COCONINO SANDSTONE. Gages at 1/2, 1, 2, and 3 inches from impact.

Table V

DRY COCONINO SANDSTONE GAGE RECORDS

Gage No.	Gage Distance from Impact (mm)	Shock Rise-Time (μsec)	Stress Amplitude (kbar)	Comments	Average Shock Velocity Between Gages (mm/μsec)
1	0	--	--	Gage shorted at impact	3.69
2	13.76	0.43*	114	Peak	
			74	Level position	
			30	Minimum	
			52	Final level position	3.64
3	28.34	0.19	90	Peak	
			45	Level position	2.69
4	53.92	0.25	31		2.32
5	78.30	0.55	26	Peak	
			16	Level position	

* Structure seen in rise.

ACKNOWLEDGMENTS

The authors thank R. W. Gates of Poulter Laboratory for assistance with the experiments using mouse-trap plane-wave generators and for help with the ultrasonic velocity measurements. We also thank Dr. H. Moore and Mr. L. E. Middlestorb of the U.S. Geological Survey for obtaining the Coconino sandstone.

REFERENCES

Ahrens, T. J., and V.G. Gregson, Jr., "Shock Compression of Crustal Rocks: Data for Quartz, Calcite, and Plagioclase Rocks," J. Geophys. Res., 69, 4839-4874, 1964.

Duvall, G. E., and G. R. Fowles, "Shock Waves," in High Pressure Physics and Chemistry, Vol. 2, ed. R.S. Bradley, Academic Press, New York, 1963.

Erkman, J. O., "Simultaneous Detonation Along a Line," Rev. Sci. Instr., 30, 818-820, 1959.

Fowles, G. R., and R. F. Williams, "Plane Stress Wave Propagation in Solids," J. Appl. Phys., 41, 360-363, 1970.

Gregson, V. G., T. J. Ahrens, and C. F. Petersen, "Dynamic Properties of Rocks," Final Report, Stanford Research Institute, Project PGU-3630, for Air Force Cambridge Research Laboratories, AFCRL-63-662, August 1963.

Keough, D. D., "Procedure for Fabrication and Operation of Manganin Shock Pressure Gages," Final Report, Stanford Research Institute, Project PGU 6979, for Air Force Weapons Laboratory, AFWL-TR-68-57, 1968.

Murri, W. J., and C.W. Smith, "Equation of State of Rocks," Interim Technical Report, Stanford Research Institute, Project PGU-6618, for U. S. Atomic Energy Commission, Lawrence Radiation Laboratory, Contract AT(04-3)-115, March 1970.

Petersen, C. F., W. J. Murri, and M. Cowperthwaite, "Hugoniot and Release Adiabat Measurements for Selected Geologic Materials," J. Geophys. Res., 75, 2063-2072, 1970.

Seaman, L., "SRI-PUFF 3 Computer Code for Stress Wave Propagation," Final Report, Stanford Research Institute, Project PGU 8152, for Air Force Weapons Laboratory, Contract F 29601-70-C-0001, 1970.